International Journal of Civil Engineering and Technology (IJCIET)
Volume 10, Issue 10, October 2019, pp. 521-536, Article ID: IJCIET_10_10_049
Available online at https://iaeme.com/Home/issue/IJCIET?Volume=10&Issue=10
ISSN Print: 0976-6308 and ISSN Online: 0976-6316
DOI: https://doi.org/10.17605/OSF.IO/2RFGM

THE CATALYTIC REDUCTION OF TOXIC DYES THROUGH PHYTO-ASSISTED SYNTHESIS OF SILVER NANOPARTICLES FROM *ERIOCAULON ODORATUM* LEAF EXTRACT

Jyotsna Akumuri*
Research Scholar (PhD), Department of Chemistry, Acharya Nagarjuna University &
Assistant Professor of Chemistry, Pragati Engineering College,
Surampalem, Andhra Pradesh, India

Dr. K. Surendra Babu
[2]Research Supervisor & Director of PG courses, SVRM College,
Nagaram, Andhra Pradesh, India
***Author for Correspondence: jyotsna.akumuri@gmail.com

ABSTRACT

This study introduces the green synthesis of silver nanoparticles using Eriocaulon odoratum leaf (E. odoratum Dalzell), a plentiful, non-toxic, and renewable Indian biomass. Silver nanoparticles (AgNPs) were synthesized from plants in a single step utilizing the aqueous extract of E. odoratum leaves (EO) and silver nitrate ($AgNO_3$) as a precursor. Transmission electron microscopy (TEM), Fourier Transform Infrared Spectroscopy (FTIR-ATR), X-Ray Diffraction (XRD), and UV-Vis Spectroscopy were used to establish the validity of the phytosynthesized AgNPs. AgNPs were successfully formed, as evidenced by the appearance of a distinctive surface plasmon resonance (SPR) absorption band with a maximum of 410 nm in the UV-vis spectroscopy examination. For up to four months, the phytosynthesized AgNPs remained stable. The presence of water-soluble biomolecules by chemical groups that may be implicated in the reduction, covering, and stability of AgNPs was confirmed by the FTIR-ATR analysis of the EO leaf extract content. AgNPs have a polycrystalline phase, according to XRD studies. With particle diameters ranging from roughly 10 to 40 nm and a mean particle size distribution of 23.06 ± 8.0 nm, TEM examination of the AgNPs confirmed their spherical form. AgNPs show catalytic activity in the reduction of the highly polluting organic dyes crystal violet (CV) and toluidine blue (TB). With only 3 and 5 minutes of reaction time, respectively, CV and TB were reduced by AgNPs in the presence of NaBH4 at room temperature. CV and TB's rate constant (k) values were calculated to be 0.3560 min^{-1} and 0.2977 min^{-1}, respectively.

Keywords: *E. odoratum* Dalzell; phytosynthesized AgNPs; Green Synthesis; Nanocatalysis; Violet crystal; toluidine blue

Cite this Article: Jyotsna Akumuri and Dr. K. Surendra Babu, The Catalytic Reduction of Toxic Dyes Through Phyto-Assisted Synthesis of Silver Nanoparticles from *Eriocaulon Odoratum* Leaf Extract. International Journal of Civil Engineering and Technology 10 (10), 2019, pp. 521-536.
https://iaeme.com/Home/issue/IJCIET?Volume=10&Issue=10

1. INTRODUCTION

Nanotechnology is a promising science for technology development. Nanoparticles are used in biomedicine, optics, and catalysis thanks to new information from chemistry, materials science, and other fields. Metallic nanoparticles are popular nanomaterials.[1] Most chemical industries use metallic catalysts to convert chemical compounds. Metallic nanoparticles are highly active catalysts due to their unique electronic properties and larger surface area. Silver nanoparticles have many industrial uses, including catalysis [2]. Their high surface area-to-volume ratio makes them attractive for reducing organic dyes. Because format, state of aggregation, size, and concentration affect nanoparticle characteristics like surface area, synthesis parameters can adjust them.

Chemical and physical synthesis produce metallic nanoparticles. These synthesis methods produce metallic nanoparticles using solvents and synthetic chemicals that may generate hazardous waste or require a lot of energy. Some researchers prefer the eco-friendly synthesis of metallic nanoparticles to reduce the use of toxic substances that may harm humans and the environment. Phytosynthesis—plant-based nanoparticle synthesis—is gaining popularity. The growing number of publications on plant-based metallic nanoparticle synthesis proves this. Plant-based nanoparticle synthesis is safer, cheaper, and greener than chemical synthesis. Plant-based nanoparticle synthesis uses whole organisms or aqueous extracts as reducing and covering agents. Biochemical extracts are essential for the phytosynthesis of metallic nanoparticles. Water-soluble phytochemicals like phenols, flavonoids, tannins, amines, amides, biopigments, and others enable nanoparticle phytosynthesis (plant-mediated synthesis) [3].

Several studies have produced metallic nanoparticles from plant extracts, including Ag, Au, Cd, and Ni.[4] India's endemic plant biodiversity could be used to make metallic nanoparticles. However, many of these plants, like *Eriocaulon odoratum* leaf (Dalzell), have yet to be used for this purpose. To our knowledge, *E. odoratum* leaf extract has not been used to synthesize catalytic metallic nanoparticles like AgNPs. Few phytochemical studies have shown that *E. odoratum* leaf extract contains phenolic compounds, flavonoids (rutin, quercetin), and tannins (epicatechin and catechin) that trigger the phytosynthesis of metallic nanoparticles.

Nanotechnology is an essential tool for scientific and technological development and can open up a world of new material possibilities. Metallic nanoparticles are examples. Due to their solubility in aqueous media, stability, and antiseptic properties, silver nanoparticles (AgNPs) have become popular in recent decades, being used in hospitals, food, textiles, and water treatment.

Successful AgNP preparation methods exist. Chemical synthesis in aqueous medium with reducing agents like hydrazine, sodium borohydride, and stabilizers like surfactants, sodium citrate, and others produces AgNPs. These reducing and stabilizing substances may be toxic to humans and the environment [5]. Thus, replacing reducing and stabilizing substances with non-toxic "green" natural substances is intriguing.

The toluidine blue dye or also called tolonium chloride, is a heterocyclic aromatic dye soluble in alcohol or water, which, in the UV-Vis spectroscopic region, has a high intensity of absorption. It is widely used in histology and in analyses to detect lesions suspected of malignancy. In addition to being a photosensitizing agent that acts very effectively in the inactivation of viruses and bacteria, pathogenic organisms. Toluidine blue solution is also used in the test to identify the presence of lignin, changing its colour from blue to pink. Chemically, this dye has a very similar structure to that of methylene blue dye, where both have similar photophysical characteristics, being in the class of triazines. Its molecular formula is $C_{15}H_{16}ClN_3S$, and its structural formula can be seen in Figure (1a) and crystal violet with molecular formula $C_{25}N_3H_{30}Cl$ in Figure 1(b)

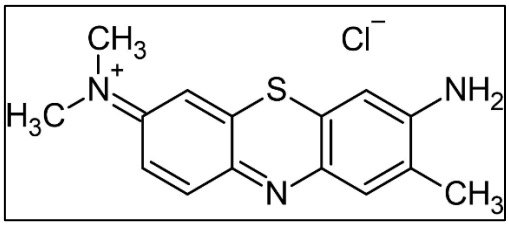

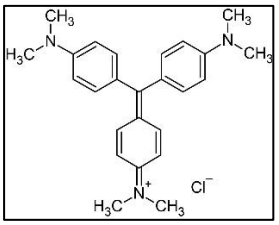

Figure 1 structures of (a): toluidine blue (TD) dye (b) crystal violet (CV) dye

The so-called ―green or ecologically friendly synthesis process uses substances of biological origin to produce metallic nanoparticles. Compared to traditional nanoparticle synthesis methods (physical and chemical), green synthesis is less harmful and has a lower operating cost. Among the substances of biological origin (biocompounds) used in the green synthesis are tannins, flavonoids, hydroxybenzoic acids, and anthocyanin, which are commonly found in the plant kingdom, including grasses such as *E. odoratum* leaf.[6] Rare literature reports on the use of *Eriocaulon* leaf biomass, specifically in studies involving nanotechnology to produce metallic nanoparticles, motivated and encouraged us to carry out this work. Giving *E. odoratum* leaf another use and a fresh scientific and technological perspective is possible if you use it in nanobiotechnology processes. In this context, the current work ingeniously demonstrates the viability of producing silver nanoparticles via green synthesis using the leaves of *E. odoratum*. In this regard, the current study suggested an easy, one-step phytosynthesis pathway using *E. odoratum* leaf (*E. odoratum* Dalzell) aqueous leaf extract for the production of AgNPs. The cationic dyes Crystal Violet (CV) and Toluidine Blue (TB) were reduced catalytically by the phytosynthesized AgNPs in the presence of sodium borohydride ($NaBH_4$) in an aqueous medium and at room temperature. Using the principles of green chemistry and green synthesis, the overall goal of the current study is to create silver nanoparticles (AgNPs) from solutions of silver nitrate salt ($AgNO_3$) and an aqueous extract of *E. odoratum* leaf (EO).

2. METHODOLOGY

This work was carried out at the Materials and Environment Laboratory, Department of Chemistry, SVRM College, Acharya Nagarjuna University.

2.1 Materials

All chemicals purchased from Sd fine, Merck & Sigma Aldrich, with AR quality, 98-99 % purity and solutions prepared with Ultrapure Water (HPLC grade).

2.1.1 Plant Material: *Eriocaulon odoratum* Dalzell (Figure 2), also known as Fragrant Pipewort [7] and Eriocaulon collinum, christopheri, and oliveri, is a plant that is native to Indo-China and India. An annual, it flourishes in the moist tropical biome. A species of grass in the Eriocaulaceae family[8] is called *E. odoratum*. Common on hills above 1300 metres in moist, shaded areas. The plants are covered in chamomil. Marsh-dwelling Fragrant Pipewort is a highly variable herb with white, spherical flowerheads carried singly atop many 35–45 cm tall leafless stems. The leaves are lance-shaped, pointed at the tip, and up to 10 x 0.3 cm in size. The stalks of flower clusters have a small, hairless limb and a sheath that can be up to 6 cm long. Floral bracts are 4 x 1.5 mm, triangular, tapering to a sharp point, and sparsely or densely hairy. Involucral bracts are 3 x 2 mm, obovate, blunt, and hyaline. Female petals are inverted-lance-shaped, hairy, and white; female sepals are 2 x 1 mm, ovate, concave, and hairy along the keel; the seed is oblong and has numerous appendages on the transverse walls. Three unequal, white petals with one larger black panther make up the male sepals, which are joined into a three-lobed, hairy sheath. Only the states of Andhra Pradesh, Karnataka, Kerala, Maharashtra, Tamil Nadu, and Sri Lanka on the peninsula of India contain fragrant pipewort. November through January is the flowering season.

Figure 2: *E. odoratum* Dalzell. (Fragrant Pipewort) plant

2.2 Preparation of Biomass: In the laboratory, the leaves of *E. odoratum* leaf were manually separated from the other parts of the plant, washed with ultrapure water (several times) to eliminate undesirable particulates, fragmented into smaller parts with the aid of scissors and dried in an oven at 60 ºC for 48 h. The dehydrated biomass (Figure 3) was then placed in an appropriate plastic bottle and kept in the absence of light until use.

2.3 Obtaining *E. odoratum* leaf aqueous extract: To obtain the aqueous extract of *E. odoratum* leaf (EO), 4 g of fragmented dry biomass were weighed on an analytical balance, which was added to 100 ml of ultrapure water at a temperature of 80ºC and kept under stirring in a rotary orbital shaker (Remi Made, India) at 150 rpm for 20 minutes [9]. After this period of time, the mixture was subjected to the filtration process with filter paper (Watman No1) and the filtrate obtained (crude extract), liquid coloured in a yellow tone (Figure 3) was used in the step of phytoreduction of the Ag^{+} ion to Ag^{0} metal and, consequently, the formation of AgNPs.

2.4 Phytosynthesis of AgNPs: The AgNPs phytosynthesis was performed in a single step using diluted silver nitrate solution ($AgNO_3$) as substrate and aqueous EO leaf extract as metal ion bioreducing agent. In one experiment, 50 mL of $AgNO_3$ solution was placed in a 125 mL Erlenmeyer on a magnetic stirrer (IKa, Germany). Then, 10 mL of fresh aqueous extract was added to this solution; the solution was kept under constant agitation (150 rpm) at a temperature of 25ºC for a certain period of time until the formation of AgNPs, confirmed by the brown colour of the solution (Figure 3). The AgNPs colloidal solution was centrifuged at 8,000G for 20 minutes (this cycle was repeated several times), the AgNPs separated, washed with ultrapure water and dried in an oven at 100oC, which were later used for characterization and catalytic studies. During AgNPs phytosynthesis, the influence of synthesis parameters such as AgNO3 concentration, extract pH and reaction time on the formation of AgNPs was investigated.

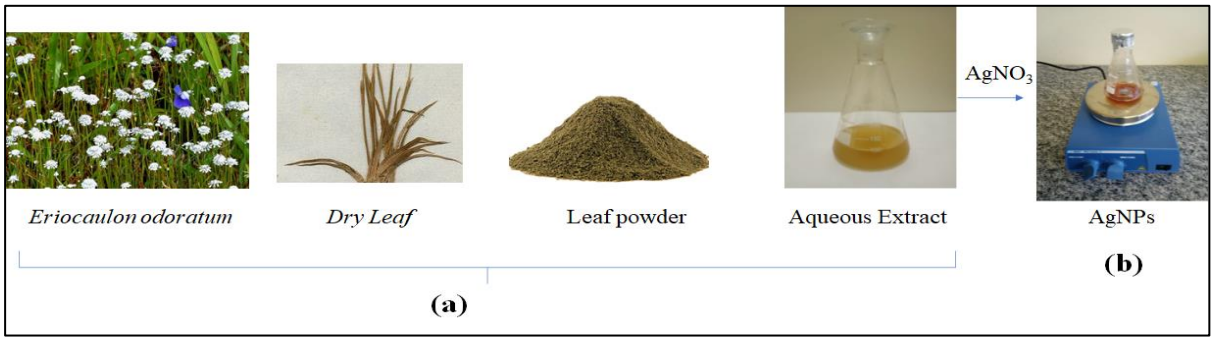

Figure 3: (a) Leaf aqueous extract obtained from *E. odoratum* leaf and (b) Obtaining AgNPs using *E. odoratum* leaf aqueous extract at room temperature

2.5 Stability study of AgNPs colloidal solution: In this experiment, the stability of the AgNPs colloidal solution was investigated. For this study, the AgNPs colloidal solution was stored under refrigeration at 5 ºC and in the absence of light, the stability was monitored using UV-Vis spectroscopy based on the variation in intensity of the SPR absorption band of the AgNPs.

2.6 Characterization of phytosynthesized AgNPs: The phytosynthesized AgNPs were characterized by the techniques of SL 159 - ELICO model ultraviolet-visible spectrophotometry (UV-Vis), Infrared spectroscopy was used for the molecular identification of secondary metabolites existing in the CA aqueous extract that may possibly be involved in the phytoreduction and stabilization of the metal ion. Analyses were performed using a Spectrum-Two FTIR spectrophotometer (PerkinElmer, USA) combined with the ATR accessory. FTIR spectra were obtained in the wavenumber region of 400–4000 cm^{-1} with a resolution of 4 cm^{-1}, accumulating 32 scans., X-ray diffraction analyses were performed using a Bruker D8 Venture diffractometer X-ray diffractometer supplied with a CuKα radiation source (λ = 1.5418 Å) and Bragg-Brentano geometry operating at a voltage of 40 kV, current of 20 mA. The 2θ angles were recorded in the 20° - 80° range at room temperature, with an integration time of 5 seconds. and Transmission electron microscopy (TEM) was used to obtain the shape, size and dispersion of AgNPs through images. TEM measurements were performed using a JEOL JEM 1400 instrument, operated at an accelerating voltage of 100 kV. AgNP diameters were measured using Sigma Pro Scan software.

2.7 Catalytic application of AgNPs: In this experiment, the catalytic activity of phytosynthesized AgNPs was investigated. Catalytic reduction studies of crystal violet (CV) and toluidine blue (TB) dyes in the presence of sodium borohydride ($NaBH_4$) and AgNPs, at room temperature were performed. In a quartz cuvette, 3 mL of dye solution (0.05M), 100 µL of a freshly prepared $NaBH_4$ solution (0.1M) and 15 mg AgNPs were placed.

The same procedure was repeated for comparison purposes except with the presence of AgNPs. The reduction of dyes by AgNPs was monitored through UV-visible spectra in the length range wavelength between 300 - 750 nm.

The percentage reduction of dyes (% R) CV and TB was calculated using the Equation 1 [10]. The kinetic reduction of CV and TB dyes was calculated using the pseudo-first-order model expressed in Equation 2

$$\% \, Removal = \frac{(Co - Ct}{Co} \times 100 \quad \text{(Eq.1)}$$

$$ln \, \frac{Cf}{Co} = -kt \quad \text{(Eq.2)}$$

Co corresponds to the initial absorbance of dyes at time zero, while Ct is the apparent absorbance of dyes at time "t" at λ_{max} = 580 nm for CV and λ_{max} = 620 nm for TB, k is the pseudo-rate constant. first order, and t is the time in minutes.

3. RESULTS AND DISCUSSIONS

3.1 Determination of the content of phenols, flavonoids and tannins in the extract

The quantitative analysis of phenols, flavonoids and tannins in the aqueous extract of the EO leaf was carried out based on the Folin-Ciocalteu methods (phenols), colourimetric method of aluminium chloride (flavonoids) and vanillin (tannins), with the purpose of obtaining the abundance of these bioactive compounds that possibly act in the phytoreduction of the metallic ion. The calculated concentrations for phenols, flavonoids and tannins in the EO aqueous extract were (103.80 ± 6.25) mg/g, (39.92 ± 4.62) mg/g and (6.25 ±0.67) mg/g respectively. These results obtained are consistent with those previously found by Costa et al. (2015) for EO extract, and some small differences can be easily associated with seasonal, environmental or genetic variations.[11]

3.2 Confirmation of the phytoreductive capacity of the extract

The ability of EO leaf aqueous extract to reduce silver ions and, consequently, to form AgNPs was investigated. The first confirmation was through visualization, considering the colour change of the extract solution, the AgNO3 solution and the extract solution containing the AgNPs. According to the literature, the change in colour of the solutions is strong evidence of the formation of AgNPs [12]. Figure 4 (inset a - b - c) shows the images of aqueous leaf extract solutions of EO, $AgNO_3$ solution (0.5 mM) and AgNPs with their characteristic colours. The extract solution has a yellow colour, and the $AgNO_3$ solution (0.5mM) is colourless. When we add the extract solution to the solution containing silver ions (Figure 4 inset b), the formation of the first AgNPs begins, and the solution remains, at first, in light yellow tones, changing to dark yellow tones and finally, becoming brown without the formation of deposited precipitates. These results confirm the phytoreduction of the Ag^+ ion to metallic Ag^0 and the formation of AgNPs. The phytochemicals in the EO extract, phenols, flavonoids and tannins acted as reducing agents of silver ions and stabilizers in the nanoparticles [13], preventing their agglomeration and precipitation in solution.

3.3 Determination of the surface plasmon resonance (SPR) absorption band of AgNPs

After visual inspection of the formation of AgNPs by the EO leaf aqueous extract, the colloidal suspension of AgNPs was subjected to UV-Vis spectroscopy analysis to determine the surface plasmon resonance (SPR) absorption band. The result of this study is shown in Figure 4. As shown in Figure 4, the AgNPs colloidal suspension exhibits an intense SPR absorption band between 350 nm and 450 nm with a wavelength (max. λ value) centred at 410 nm. According to the literature, AgNPs present a characteristic SPR absorption band in the range between 320-

460 nm [12]. Therefore, the results obtained in the UV-Vs analysis confirm the occurrence of AgNPs by EO extract. The SPR band profile indicates that AgNPs are possibly spherical [12-13]. This result was corroborated by the MET analysis.

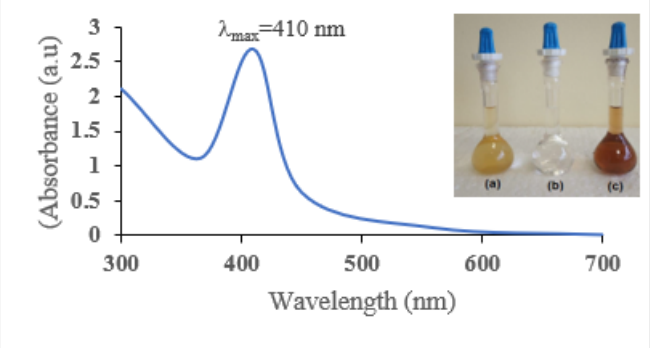

Figure 4: UV-vis absorption spectrum of colloidal AgNPs solution.

3.4 Study of the influence of phytosynthesis parameters

After confirming the phytoreduction capacity of the extract and the characterization of the AgNPs SPR band, experiments were carried out to verify the influence of the synthesis parameters with AgNO3 concentration, extract pH and reaction time in the formation of AgNPs, in order to optimize their preparation. The experiments are described below.

3.4.1 Influence of $AgNO_3$ concentration

The influence of $AgNO_3$ concentration on the formation of AgNPs was evaluated. The $AgNO_3$ concentration was varied from 0.25 mM to 2 mM, maintaining the extract's natural pH (pH~5). Figure 5 shows the results of these studies. Figure 5 (a) shows the profiles of the absorption spectra of the phytosynthesized AgNPs solutions with different concentrations of AgNO3. Analyzing Figure 5, the dependence of the AgNO3 concentration on the formation of AgNPs can be verified. Analyzing the profiles of the SPR absorption bands of the AgNPs, it is verified that when the $AgNO_3$ concentration increases from 0.25 mM to 2 mM, their SPR absorption bands increase in intensity, probably indicating that more AgNPs are produced. In addition, with the increase in $AgNO_3$ concentration from 0.25 mM to 2 mM, a shift (redshift) of the characteristic SPR absorption bands from 410 nm to 430 nm is observed, suggesting the hypothesis of an increase in the size of AgNPs with the increased concentration of $AgNO_3$. These results obtained are in good agreement with those previously observed by others in the green synthesis of AgNPs using *ergenia Ciliata*, *Clitoria Ternatea*, *Cochlospermum Religiosum*, *Dianthus Caryophyllus*, *Garcinia Mangostana*, *Hyacinthus Orientalis*.[14] It is concluded from these results that 0.50 mM of AgNO3 is considered the adequate concentration for converting the precursor into nanoparticles. Figure 5 (b) shows the images of the phytosynthesized AgNPs solutions with different concentrations of $AgNO_3$. As shown in Figure 5, the colours of the AgNP solutions varied with the concentration of $AgNO_3$ used. The greater the increment of $AgNO_3$, the more intense the staining of the solutions, suggesting a greater amount of AgNPs formed.

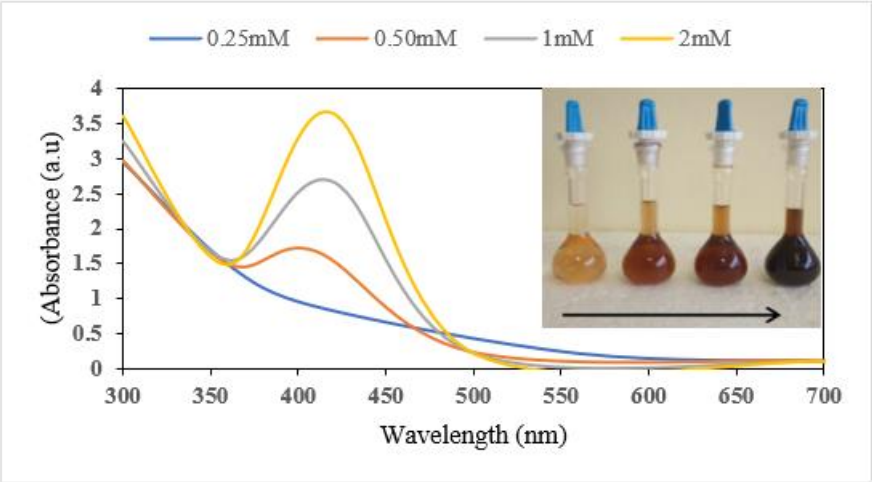

Figure 5: UV-Vis spectra (a) AgNPs phytosynthesized with different concentrations of $AgNO_3$ (from left to right), and (inset) images of the respective solutions

3.4.2 Influence of extract pH

The influence of the pH of the EO extract on the formation of AgNPs was studied at pH 2 and 4 (acidified solution), pH 7 (neutrality), and at pH 8 and 10 (basic solution). The pH values of the extract were adjusted with 0.1 M HCl and 0.1 M NaOH solutions with the aid of a digital pH meter (Elico, India). The results of these studies are shown in Figure 6 (a – b).

Figure 6 (a) shows that a more intense SPR signal was obtained for the reaction at pH 8 (slightly basic medium), probably indicating that more AgNPs are formed, while at pH 2 (very acidic pH value), AgNPs are not formed. were formed (absence of SPR band). These results can be explained by considering the change in the loads of phytochemicals in the EO extract with a change in the pH of the extract. A presumptive hypothesis for this behaviour is that at pH 8 (slightly basic pH value), the EO leaf extract may contain more negatively charged functional groups capable of efficiently reducing Ag+ than at pH 2, 4 and 7. At pH 2.0 (very acidic), EO leaf extract mainly contains positively charged functional groups with a low ability to bind and reduce Ag+; for this reason, AgNPs are not formed. Another alternative possibility is that the chemical base used to adjust the pH of the extract to higher values could directly increase the Ag+ reduction and positively influence the synthesis yield. Otherwise, the acid to lower the pH could dissolve some AgNPs or prevent Ag0 from meeting and ionizing these neutral atoms. Furthermore, Figure 6(a) reveals that when AgNPs phytosynthesis is carried out at pH 10, there is a significant decrease in the SPR absorption band at 410 nm due to some tendency to agglomeration of AgNPs. Similar effects of pH on AgNPs phytosynthesis have been reported by other authors [15]. Based on these obtained results, it is concluded that the ideal condition for AgNPs phytosynthesis is at pH 8. Figure 6 (b) shows the images of the phytosynthesized AgNPs solutions at different pH of the extract.

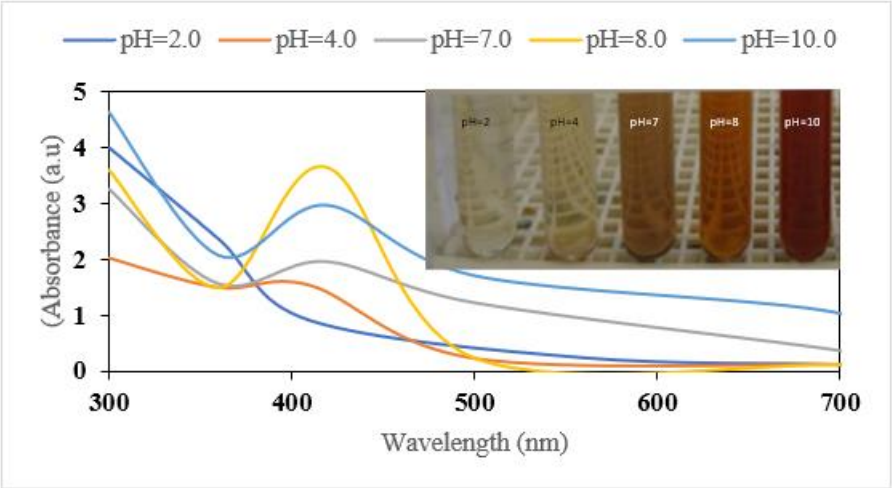

Figure 6: UV-Vis spectra (a) AgNPs phytosynthesized at different pH and (inset) images of the respective solutions

3.4.3 Influence of reaction time

The influence of reaction time on AgNPs phytosynthesis was studied. Reaction times were varied from 1h to 12 h, using 0.50 mM $AgNO_3$ and extract pH adjusted to 8. The results of these studies are shown in Figure 7 (a - b). According to the spectral profiles obtained, the reaction time interferes in the stage of the AgNPs formation process. As the reaction time increases from 1 h to 6 h, the intensity of the SPR absorption band at 410 nm also increases, suggesting that greater amounts of AgNPs are produced. These results showed that the necessary reaction time for forming AgNPs from $AgNO_3$ is 6h. For phytosyntheses carried out with times greater than 6h, no significant variation was observed in the intensity of the SPR absorption band at 410 nm, as shown in Figure 7 (b), confirming the complete formation of AgNPs with 6h. Thus, the reaction time of 6h was adopted as the best condition for AgNPs phytosynthesis.

Considering the influences of $AgNO_3$ concentration, pH of the extract and reaction time, the optimized conditions for the phytosynthesis of AgNPs by the EO extract were selected as follows: $AgNO_3$ 0.5 mM, extract pH 8 and reaction time of 6 h. For subsequent stability, characterization and application studies, phytosynthesized AgNPs were used under optimized conditions.

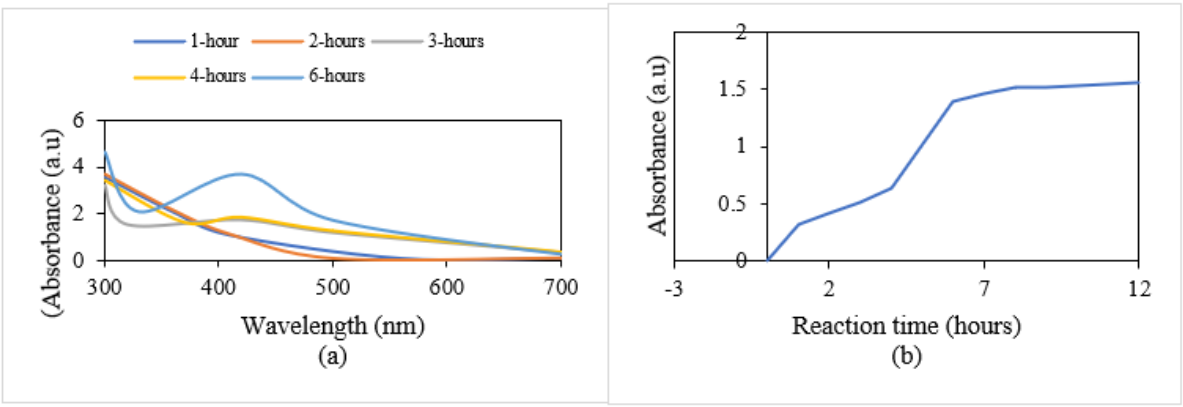

Figure 7: UV-Vis spectra (a) AgNPs phytosynthesized at different reaction times and (b) variation of the intensity of the absorption band with the reaction time for the formation of AgNPs.

3.5 Stability of AgNPS colloidal solution

The stability of the colloidal solution of phytosynthesized AgNPs was studied through UV-Vis spectroscopy. The profiles of the SPR spectra of AgNPs phytosynthesized on the day and after some time were compared. These results are shown in Figure 8. As shown in Figure 8, the SPR with λ_{max} centred at 410 nm [12] remained practically unchanged after four months, suggesting that there was no notable variation in the optical properties and probably in the structural characteristics of the AgNPs. Furthermore, only a slight difference in absorption intensity of the SPR band was observed, suggesting that the phytochemicals (phenols, flavonoids and tannins) from the EO leaf aqueous extract form a stabilizing layer on the surface of AgNPs, avoiding their agglomeration. Phytosynthesized AgNPs remained stable after four months of storage, which can be considered a positive factor for making them long-term use.

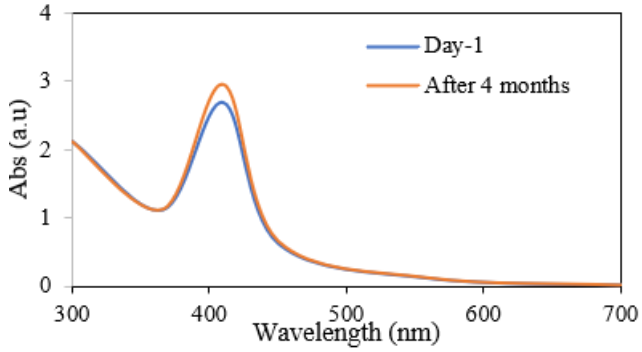

Figure 8: UV-Vis spectra of phytosynthesized AgNPs at pH=8, stored under refrigeration and in the absence of light.

3.6 Characterization of phytosynthesized AgNPs

3.6.1 Fourier Transform Infrared Spectroscopy Analysis - (FTIR)

Fourier transform infrared spectroscopy (FTIR-ATR) was used to identify the chemical groups of bioactive molecules from the EO extract that are possibly involved in the phytoreduction of metal ions and stabilization of AgNPs. FTIR-ATR measurements of the EO extract and EOAgNPs obtained after the centrifugation and drying process were carried out. The spectroscopic results of these studies are shown in Figure 9.

Figure 9 (a) refers to the EO extract spectrum and shows absorption bands between 828 cm^{-1} and 3294 cm^{-1} referring to chemical groups associated with phenols, flavonoids, tannins and proteins. The intense band at 3294 cm^{-1} in the spectrum was attributed to alcohol and phenol (-OH) groups. The smaller band in the region of 2926 cm^{-1} indicates alkane compounds (-CH). The intense band at 1565 cm^{-1} is a amide I (-NHCO) characteristic. The absorption band at 1400 cm^{-1} may be due to the asymmetric and symmetric elongation of the carboxylate ions (-COO-). The intense band at 1037 cm^{-1} denotes the elongation vibration of the ether (-COC), ester (-COO) and carboxylic (-COOH) groups[16]. The lowest absorption band at 828 cm^{-1} was attributed to alkenes and aromatic rings (-CH) groups. The FTIR-ATR spectrum of the EOAgNPs (Figure 9(b)) shows significant similarity with the EO extract spectrum. When comparing the EO extract spectrum with the EOAgNPs spectrum, some changes in the absorption bands can be observed. The interaction of AgNPs with the phytochemical molecules in the extract changes the spectrum of EOAgNPs. These changes are a decrease in intensity, widening and disappearance of the band. The band at 3294 cm^{-1} observed in the EO extract in relation to the phenol (-OH) groups was wider and shifted to 3288 cm^{-1}. The band at 2931 cm^{-1} was shifted to 2926 cm^{-1}, and a new band at 2954 cm^{-1} was observed.

The intensity of the absorption band at 1565 cm^{-1} relative to amide I (-NHCO) was decreased and the band was shifted to 1633 cm^{-1}. The intense band at 1405 cm^{-1} corresponding to elongation (-COO-) was split into two bands at 1457 cm^{-1} and 1365 cm^{-1}. The band at 1037 cm^{-1} corresponding to the ether (-COC), ester (-COO) and carboxylic (-COOH) groups decreased in intensity and was shifted to 1040 cm^{-1}. The band at 828 cm^{-1} corresponding to alkenes and aromatic ring groups (-CH) disappeared. Based on these FTIR results, it is possible to conclude that biomolecules with functional groups such as -OH, -NHCO, -CO, -COC and -COOH are involved in reducing phytosynthesized AgNPs.

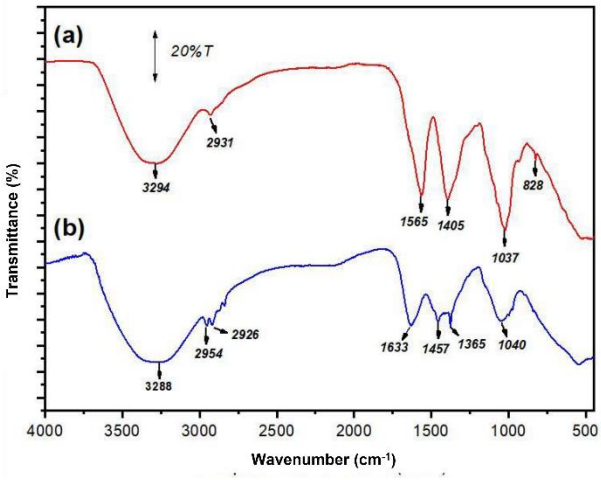

Figure 9: Fourier transform infrared absorption spectra of (a) EO extract and (b) EOAgNPs.

Based on the results obtained in the FTIR analysis, a simplified hypothetical scheme involving the phytoreduction and stabilization of AgNPs by the bioactive molecules of the EO aqueous extract is proposed in Figure 10. In this proposed hypothesis, the flavonoid compounds of the EO extract would act as oxidizing agents being oxidized by $AgNO_3$, consequently resulting in the formation of AgNPs. Phenolic compounds containing ketones and hydroxyls can bind to metal ions and reduce $AgNO_3$; proteins can interact with AgNPs and come to coat them.

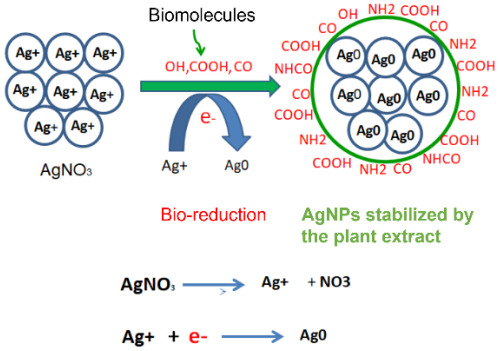

Figure 10: Phytoreduction and stabilization of AgNPs by extract biomolecules.

3.6.2 X-ray Diffraction Analysis - (XRD)

X-ray diffraction analysis (XRD) was used to characterize the crystalline nature of AgNPs. The results obtained from this analysis are shown in Figure 11. Figure 11 reveals four distinct Bragg peaks at 2θ = 38°, 46°, 65° and 78° values that correspond to the diffraction peaks of the face-centred cubic crystalline plane (CFC) of Ag from (111), (200), (220) and (311). These 2θ values obtained for silver are in agreement with the lattice constant (JCPDS card nº 4-0783) for the standard pure Ag diffractogram. These results confirm the polycrystalline phase of phytosynthesized AgNPs.

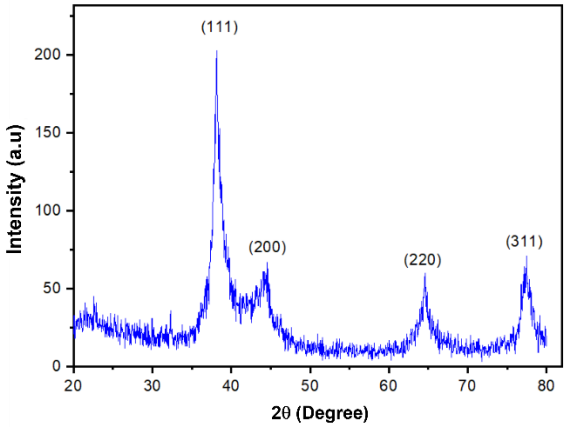

Figure 11: X-ray diffractogram of AgNPs.

3.6.3 Transmission Electron Microscopy Analysis - (TEM)

TEM analysis was conducted to characterize the AgNPs in terms of shape, size and state of aggregation. The results of this analysis are shown in Figures 12a & b. Figure 12a shows the TEM image of the phytosynthesized AgNPs. As shown in Figure 12a, AgNPs are spherical particles with moderate particle size variation and aggregated.

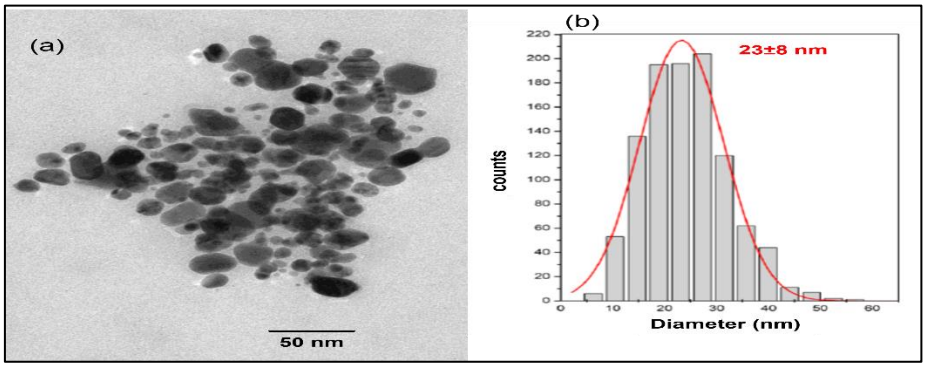

Figure 12: (a) TEM Micrograph of the phytosynthesized AgNPs and (b) Histogram with the size distribution of AgNPs.

Figure 12b refers to the TEM-based particle size distribution histogram. The AgNPs show that the diameters of the AgNPs range from 10 to 40 nm, with an average particle size of 23.06 ± 8.0 nm.

3.7 Catalytic application of AgNPs

The catalytic activity of phytosynthesized AgNPs was investigated in the reduction of Crystal Violet (CV) and Toluidine Blue (TA) in an aqueous medium, in the presence of $NaBH_4$, and at room temperature. The decline in colour intensity of the dye solutions was used to confirm whether the reduction processes were successful. The results of these tests are shown in the following Figures. The absorption spectrum of CV reduction (λ_{max} 580 nm) [17]at different reaction times is shown in Figure 13. As can be seen in Figure 13. Figure 13, with 3 min of reaction time, the intensity of the absorption band at 580 nm decreased substantially and practically disappeared due to the change from the characteristic violet colour of CV to colourless (leuco). These results indicate that the reduction of CV by AgNPs was completed within 3 minutes. The calculated per cent reduction (%R), using Equation 1, was 99.16 ± 0.53% for the 3 min time. The reduction in CV dye kinetics was monitored and calculated using the pseudo-first-order model (Equation 1).

The result of the linear regression graph of log absorbance (lnA) of CV (580 nm) versus reaction time (t) is shown in Figure 13a. Figure 13b shows a good linear correlation (R^2= 0.9898) between the graph of lnA versus t. The value of the calculated rate constant (k) was 0.3560 min^{-1}. Images of CV dye solutions (0.05 M) before and after reduction with NaBH4 and AgNPs are shown in inset.

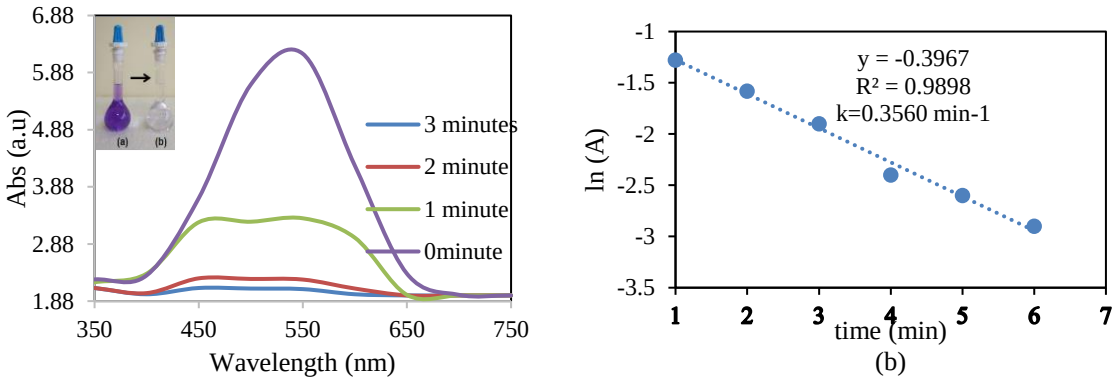

Figure 13 (a) UV-vis spectra of the catalytic reduction of CV with $NaBH_4$ and AgNPs at different times. (b) Linear regression graph of logarithm of absorbance (lnA) versus time of CV reduction in the presence of $NaBH_4$ and without AgNPs and (inset) CV dye solutions (0.05M), (a) before and (b) after reduction with $NaBH_4$ and AgNPs.

The UV-visible absorption spectra, referring to the reduction of the TB dye (λmax 620 nm) at different reaction times, are shown in Figure 14. As shown in Figure 14, the absorption intensity band at (λ_{max}) 620 nm of the TB dye gradually decreased with increasing reaction time up to 5 min, when the absorption band practically disappeared due to the characteristic colour change of blue TB, changing to colourless. These results indicate that about 5 min is the required reaction time to reduce the dye. The per cent reduction (%R) for the TB dye was calculated using Equation 1. Based on Equation 1, the calculated %R values were 99.35 ± 0.32% for the time in 5 min. The reduction of TB dye kinetics was monitored and calculated using the pseudo-first-order model (Equation 2). The result of the linear regression graph of the logarithm of absorbance (lnA) of TB (620 nm) versus reaction time (t) is shown in Figure 14b and shows a good linear correlation between the plot of lnA versus t. The value of the calculated rate constant (k) was 0.2977 min^{-1}.

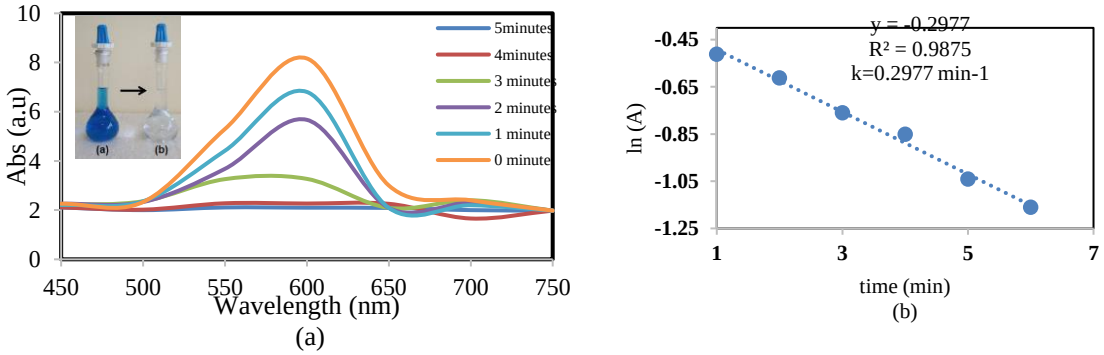

Figure 14: (a) UV-vis spectra of the catalytic reduction of TB with $NaBH_4$ and AgNPs at different times. (b) Linear regression graph of logarithm of absorbance (lnA) versus time (t) of TB reduction in the presence of $NaBH_4$ and AgNPs. (inset) TB dye solutions (0.05M), (a) before and (b) after reduction with $NaBH_4$ and AgNPs.

Images of TB dye solutions (0.05 M) before and after reduction with $NaBH_4$ and AgNPs are shown in Figure 14a (inset). A study similar to the one described above was carried out; however, the results obtained were compared only with $NaBH_4$ and in the absence of AgNPs. The results of these experiments are shown in Figures 15a, b. The UV-visible absorption spectra, referring to the reduction of the CV dye (λ_{max} 580 nm) at different reaction times in the presence of $NaBH_4$, the absence of Figure 15a shows the AgNPs and the ambient temperature. When analyzing Figure 15a, it is evident that the CV reduction reaction in the absence of AgNPs was slower when compared to that in the presence of AgNPs, confirming the role of phytosynthesized AgNPs as promoters' efficiency in electron transfer between NaHB4 and dye molecules during the reduction reaction. The results of the linear regression plot of log absorbance (lnA) of CV (580 nm) versus reaction time (t) with $NaBH_4$ only in the absence of AgNPs are presented in Figure 15a. The result inserted in Figure 15b shows that the values of the rate constant (k) obtained for CV (k = 0.0293 min^{-1}) in the absence of AgNPs. It is much smaller when compared with those values of rate constant (k) obtained for CV (k = 0.3560 min^{-1}) in the presence of AgNPs. This data demonstrates that the CV reduction reaction in the absence of AgNPs was slower when compared to that in the presence of AgNPs.

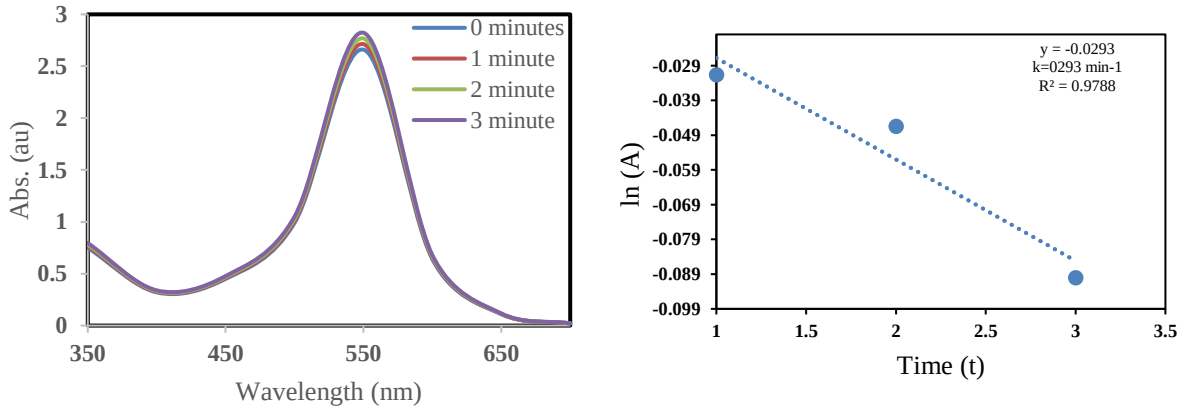

Figure 15: (a) UV-vis spectra of catalytic reduction of CV with $NaBH_4$ and absence of AgNPs at different times (b) Linear regression graph of logarithm of absorbance (lnA) versus time of CV reduction in the presence of $NaBH_4$ and without AgNPs.

The UV-visible absorption spectra, referring to the reduction of the TB dye (λmax 620 nm) at different reaction times in the presence of $NaBH_4$, the absence of AgNPs, and at room temperature, are shown in Figure 16a. The result of the graph linear regression of the logarithm of absorbance (lnA) of TB (620 nm) versus reaction time (t) only with $NaBH_4$ in the absence of AgNPs can be observed in Figure 16b. The result inserted in Figure 16(b) shows that the value of the constant of rate (k) obtained for TB (k = 0.0151 min^{-1}) in the absence of AgNPs is much smaller than when compared with those rate constant values (k) obtained for TB (k = 0.2977 min^{-1}) in the presence of AgNPs. This data demonstrates that the TB reduction reactions in the absence of AgNPs were slower when compared to those in the presence of AgNPs. The result obtained confirms the role of phytosynthesized AgNPs as efficient promoters of electron transfer between NaHB4 and dye molecules during the reduction reaction.

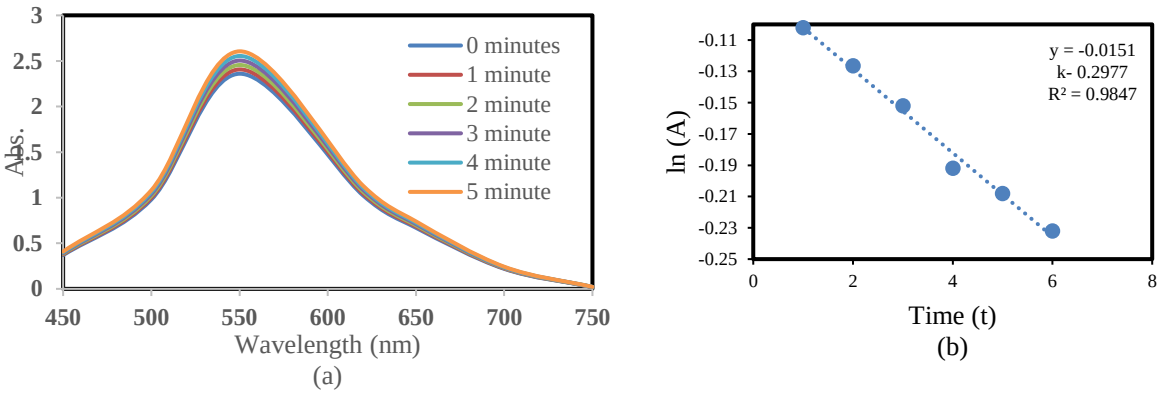

Figure 16: (a) UV-vis spectra of the catalytic reduction of TB with $NaBH_4$ and absence of AgNPs at different times. (b) Linear regression graph of the logarithm of absorbance (lnA) versus time of TB reduction in the presence of $NaBH_4$ and without AgNPs.

Based on the results presented in this paper, we can conclude that phytosynthesized AgNPs exhibit catalytic activity in the reduction of CV and TB dyes, both highly polluting organic compounds.

CONCLUSIONS

The aqueous leaf extract of *E. odoratum* leaf can be used as a reducing and stabilizing agent to obtain silver nanoparticles (AgNPs) from $AgNO_3$ through green synthesis. The phytosynthesized AgNPs have crystalline nature, spherical shapes and average particle size of 23.06 ± 8.0 nm and with a plasmonic resonance band at 410 nm. The colloidal solution of the produced nanoparticles showed stability for up to four months. The nanoparticles show excellent catalytic activity in the reduction of crystal violet and toluidine blue dyes in the presence of $NaBH_4$ and at room temperature. Considering the results achieved in this work, it is concluded that *E. odoratum* leaf, a non-toxic and abundant plant biomass, proved to be an excellent alternative for obtaining silver nanoparticles using the green and ecologically friendly method. The prepared nanoparticles have great potential for use in catalytic processes for decolorizing water-containing cationic dyes.

REFERENCES

[1]. Mobasser, Shariat & Firoozi, Ali Akbar. (2016). Review of Nanotechnology Applications in Science and Engineering. *Journal of Civil Engineering and Urbanism*, 6. 84-93.

[2]. Beyene, Hayelom & Werkneh, Adhena & Bezabh, Hailemariam Kassa & Gebregiorgis Ambaye, Teklit. (2017). Synthesis paradigm and applications of silver nanoparticles (AgNPs), a review. *Sustainable Materials and Technologies*. 13. 10.1016/j.susmat.2017.08.001.

[3]. Goswami, Monmi & Baruah, Debjani & Das, Archana. (2018). Green synthesis of silver nanoparticles supported on cellulose and their catalytic application in scavenging of organic dyes. *New Journal of Chemistry*. 42. 10.1039/C8NJ00526E.

[4]. Babaladimath, Gangadhar & Badalamoole, Vishalakshi. (2019). Silver nanoparticles embedded pectin-based hydrogel: a novel adsorbent material for separation of cationic dyes. *Polymer Bulletin*. 76. 10.1007/s00289-018-2584-7.

[5]. Hassan, Ahmed & Ewais, H.A. & Basaleh, Amal. (2017). Silver nanoparticles immobilised on the activated carbon as an efficient adsorbent for the removal of crystal violet dye from aqueous solutions. A kinetic study. *Journal of Molecular Liquids*. 248. 833-841. 10.1016/j.molliq.2017.10.109.

[6]. Hassanpour, Shahin & Maheri-Sis, Naser & Eshratkhah, Behrad & baghbani mehmandar, Farhad. (2011). Plants and secondary metabolites (Tannins): A Review. *Int. J. Forest, Soil and Erosion.* 1. 47-53.

[7]. Arisdason, W. 2011. Eriocaulon odoratum. In: IUCN 2011. IUCN Red List of Threatened Species. Version 2011.2. <www.iucnredlist.org>.

[8]. Sankara Rao, K., Arun Singh R., Deepak Kumar, Raja K Swamy and Navendu Page (2016). Digital Flora of Eastern Ghats.

[9]. Ahuja, S., and Diehl, D. 2006. Sampling and Sample Preparation. In: Comprehensive Analytical Chemistry,Vol. 47 (Eds.), S Ahuja, and N Jespersen, Oxford, UK: Elsevier (Wilson & Wilson) Chap-2, pp.15-40

[10]. Idan, Intidhar & Md Jamil, Siti Nurul Ain & Luqman Chuah, Abdullah & Choong, Thomas. (2017). Removal of Reactive Anionic Dyes from Binary Solutions by Adsorption onto Quaternized Kenaf Core Fiber. *International Journal of Chemical Engineering*. 1-13. 10.1155/2017/9792657.

[11]. Costa, Romero & Vaz, Antônio & Xavier, Haroudo & Correia, Maria & Carneiro-da-Cunha, Maria. (2015). Phytochemical screening of *Phthirusa pyrifolia* leaf extracts: Free-radical scavenging activities and environmental toxicity. *South African Journal of Botany*. 99. 10.1016/j.sajb.2015.03.193.

[12]. Zargar, Behrooz & Hatamie, Amir. (2012). Colorimetric determination of resorcinol based on localized surface plasmon resonance of silver nanoparticles. *Analyst.* 137. 5334-8. 10.1039/c2an35504c.

[13]. Raja, Bothi & Rahim, Afidah & Qureshi, Ahmad Kaleem & Awang, Khalijah. (2014). Green synthesis of silver nanoparticles using tannins. *Materials Science-Poland*. 32. 10.2478/s13536-014-0204-2.

[14]. Ana-Alexandra, Sorescu & Nuta, Alexandrina & Ion, Rodica-Mariana & Suica-Bunghez, Ioana-Raluca. (2016). Green synthesis of silver nanoparticles using plant extracts. 10.18638/scieconf.2016.4.1.386.

[15]. Ider, Mina & Abderrafi, Kamal & Eddahbi, Adil & Ouaskit, Said & Kassiba, Abdelhadi. (2017). Silver Metallic Nanoparticles with Surface Plasmon Resonance: Synthesis and Characterizations. *Journal of Cluster Science*. 28. 10.1007/s10876-016-1080-1.

[16]. Tang, Hailong & Pu, Zejun & Huang, Xu & Wei, Junji & Liu, Xiaobo & Lin, Zhiqun. (2014). Novel blue-emitting carboxyl-functionalized poly(arylene ether nitrile)s with excellent thermal and mechanical properties. *Polym. Chem*.. 5. 10.1039/C3PY01782F.

[17]. Rauf, Muhammad & Qadri, Shahnaz & Ashraf, Sarmadia & Mansoori, Miswahul. (2009). Adsorption Studies of Toluidine Blue from Aqueous Solutions onto Gypsum. *Chemical Engineering Journal*. 150. 90-95. 10.1016/j.cej.2008.12.008.